Magazine of Concrete Research
Volume 68 Issue 22

Cyclic constitutive model for strain-hardening cementitious composites
Wu, Pan and Meng

Magazine of Concrete Research, 2016, **68**(22), 1133–1142
http://dx.doi.org/10.1680/jmacr.15.00052
Paper 1500052
Received 27/01/2015; revised 25/12/2015; accepted 19/02/2016
Published online ahead of print 29/03/2016
Keywords: cement/cementitious materials/finite element methods/strain

ice
Institution of Civil Engineers
publishing

Cyclic constitutive model for strain-hardening cementitious composites

Chang Wu
PhD Student, School of Civil Engineering, Southeast University, Nanjing, China

Zuanfeng Pan
Assistant Professor, College of Civil Engineering, Tongji University, Shanghai, China (corresponding author: zfpan@tongji.edu.cn)

Shaoping Meng
Professor, School of Civil Engineering, Southeast University, Nanjing, China

A uniaxial cyclic constitutive model for strain-hardening cementitious composites (SHCCs) is proposed based on the response of the material at the stress–strain level under different loading regimes. The ascending branch of the compressive envelope curve was developed using the form of a parabolic curve, while the descending branch adopted the bilinear form. The full tensile stress–strain curve was approximately simulated by a trilinear form comprising ascending, strain-hardening and descending branches. Using the method of setting a reference point, the characteristics of the unloading and reloading process were determined, with consideration of the partial unloading–reloading scheme. Furthermore, the transition between tension and compression was taken into account in the model development. The proposed cyclic constitutive model was coded into the OpenSees platform and applied to simulate the responses of specimens at material and member levels. The simulation results indicate that the proposed model is reasonably accurate in simulating the mechanical properties of SHCC material and the cyclic behaviour of SHCC flexural elements.

Notation

E	Young's modulus
E_r	slope of reloading line
f_c	peak stress
f_{cu}	residual stress
f_{t0}	cracking stress
f_{t1}	peak tensile stress
k	shape factor of ascending branch
ε_c	compressive strain at peak stress f_c
ε_{cmin}	minimum experienced compressive strain
ε_{cu}	strain corresponding to f_{cu}
ε_{tmax}	maximum experienced tensile strain
ε_{tu}	ultimate tensile strain
ε_{t0}	strain corresponding to f_{t0}
ε_{t1}	strain corresponding to f_{t1}
ε_{us}	strain at unloading point
σ_{com}	compressive stress
σ_{cmin}	corresponding stress to ε_{cmin}
σ_{ten}	tensile stress
σ_{tmax}	corresponding stress to ε_{tmax}
σ_{us}	stress at unloading point

Introduction

There are enormous numbers of applications of concrete in infrastructure construction throughout the world. However, due to concrete's low tensile strength, low toughness and the uncontrollability of crack widths, problems of accumulative damage and catastrophic behaviour of concrete structures can occur under severe environments or during earthquake loading. Since the early 1960s, various fibres (e.g. steel, glass, carbon, synthetic and natural fibres) have been added to cementitious composites to improve their mechanical performance, and these types of composites are well known as fibre reinforced cementitious composites (FRCCs). Among the various classes of FRCCs that have been developed, a particular class of generally moderate tensile strength but with strain-hardening behaviour, called strain-hardening cementitious composites (SHCCs), has gained ground in both research and applications. Unlike the crack localisation and tension-softening behaviours of normal FRCCs, SHCCs – composite materials comprising a cement-based matrix and short reinforcing fibres – are highly ductile materials that exhibit multiple fine cracks and pseudo strain-hardening characteristics under uniaxial tensile stress. SHCC characteristics have been achieved with moderate fibre contents in engineered cementitious composites (ECCs). ECCs, developed by Li and Leung (1992) and Li *et al.* (1993) based on the basic principle of micromechanics and fracture mechanics, consist of cement, mineral admixture, fine aggregates (maximum grain size usually 0·15 mm), water, admixtures to enhance strength and workability, and less than 2% volume of short fibres. ECCs

exhibit multiple cracks formed uniformly over the length of the specimen, and the opening of each crack is usually controlled to be less than 100 μm; consequently, the ultimate tensile strain can reach over 2·0% with less than 2% volume of fibres.

Over the past two decades, SHCC materials with excellent tensile performance, high energy dissipation capacity and good durability have attracted the attention of many researchers and designers. Research efforts have focused on the micromechanics (Lee *et al.*, 2010), interface tailoring (Li *et al.*, 2002), mechanical properties (Hou *et al.*, 2012; Yun *et al.*, 2007), seismic behaviour (Kesner and Billington, 2005; Parra-Montesinos and Wight, 2000) and durability (Yun *et al.*, 2011). Because the ductility and durability of SHCCs are significantly greater than those of conventional concrete, attempts are being made to replace conventional concrete with SHCCs in structures in high-intensity earthquake regions or under severe environmental conditions. Some fairly recent applications of SHCCs include precast SHCC coupling beams, which were used to connect core walls in Japan (Maruta *et al.*, 2005), SHCC link slabs for replacing a conventional bridge deck expansion joint in Michigan, USA (Keoleian *et al.*, 2005) and surface repair of concrete structures in Japan (Kojima *et al.*, 2004).

The constitutive model under uniaxial reverse load conditions is one of the most basic mechanical characteristics of SHCCs and is the foundation for seismic non-linear analysis. To date, very few cyclic loading experiments and few cyclic constitutive models for SHCCs have been reported. Fukuyama *et al.* (1999) investigated the tension–compression behaviour of SHCC material with polyvinyl alcohol fibres. Kesner *et al.* (2003) examined the response of SHCCs to uniaxial monotonic and cyclic loading. The cyclic testing indicated that results from monotonic uniaxial tension and compression tests could be used to provide input parameters (i.e. modulus of elasticity, peak stress and peak strain) for cyclic modelling of SHCC using uniaxial stress–strain data, provided that the compressive strength of the material was not expected to be exceeded. Fischer and Li (2002) studied the effect of ductile deformation behaviour of SHCCs on the response of steel reinforced flexural members to lateral load reversals. Han *et al.* (2003) proposed a constitutive model based on total strain to simulate the uniaxial reversed cyclic experiment reported by Kesner and Billington (2001). However, the compressive envelope curve in the model of Han *et al.* (2003) was assumed to be of bilinear form, which might be incompatible with reality, and the transition between tension and compression was not considered in the cyclic model. Gencturk and Elnashai (2013) developed a cyclic constitutive model for SHCC materials based on the study of Han *et al.* (2003), and this model was implemented into Zeus NL software (Elnashai *et al.*, 2010). However, the model is relatively complicated and it is difficult to port the model code across various platforms.

A uniaxial cyclic constitutive model for SHCC materials is proposed in this paper. The ascending branch of the compressive envelope curve was developed using the form of a parabolic curve, while the bilinear form was adopted for the descending branch of the curve. A trilinear form was used to simulate the ascending, strain-hardening and descending branches of the tensile stress–strain curve. Using the method of setting a reference point, the characteristics of the unloading and reloading process were determined, with consideration of the partial unloading–reloading scheme. Furthermore, the transition from tension to compression or from compression to tension was considered in the cyclic model. The proposed cyclic constitutive model was coded into the OpenSees platform (OpenSees, 2014) and the proposed model was validated at the stress–strain level and the member level with OpenSees programming.

Cyclic constitutive model for SHCC

Backbone curves

A backbone curve is constructed by joining the points with the maximum absolute value of stress at every strain value in the loading history. A monotonic curve can be taken as the backbone curve for simplicity and ease in determination of the model parameters (Bahn and Hsu, 1998; Gencturk and Elnashai, 2013; Han *et al.*, 2003; Yankelevsky and Reinhardt, 1989).

Tensile stress–strain curve

Monotonic tests performed on SHCC material indicate that the tensile behaviour is characterised by three distinct branches consisting of a linear elastic stage, a pseudo strain-hardening stage and a tension-softening stage (Han *et al.*, 2003), as shown in Figure 1. Once the tensile strain exceeds ε_{tu}, the SHCC material is unable to sustain any tensile stresses. The expression for the tensile stress–strain relationship is

$$1.\quad \sigma_{ten} = \begin{cases} E\varepsilon & (\varepsilon \le \varepsilon_{t0}) \\ f_{t0} + (f_{t1} - f_{t0})\left(\dfrac{\varepsilon - \varepsilon_{t0}}{\varepsilon_{t1} - \varepsilon_{t0}}\right) & (\varepsilon_{t0} < \varepsilon \le \varepsilon_{t1}) \\ f_{t1}\left(\dfrac{\varepsilon - \varepsilon_{tu}}{\varepsilon_{t1} - \varepsilon_{tu}}\right) & (\varepsilon_{t1} < \varepsilon \le \varepsilon_{tu}) \\ 0 & (\varepsilon > \varepsilon_{tu}) \end{cases}$$

in which E is Young's modulus, f_{t0} and f_{t1} represent the cracking stress and peak tensile stress of the SHCC material, respectively, ε_{t0} and ε_{t1} are the strains corresponding to f_{t0} and f_{t1}, respectively, and ε_{tu} is the ultimate tensile strain.

Compressive stress–strain curve

Many constitutive laws for concrete under uniaxial compression have been proposed, but the model proposed by Hognestad *et al.* (1955) is widely used. The ascending branch of the compressive envelope curve was developed using the form of a parabolic curve, while the bilinear form was adopted

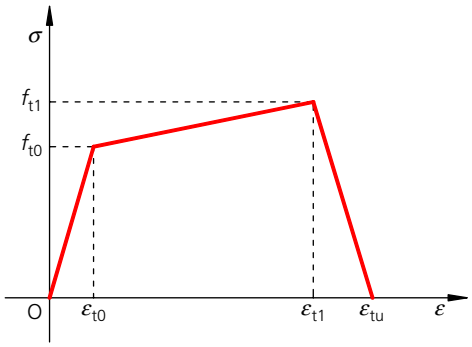

Figure 1. Uniaxial tensile stress–strain curve

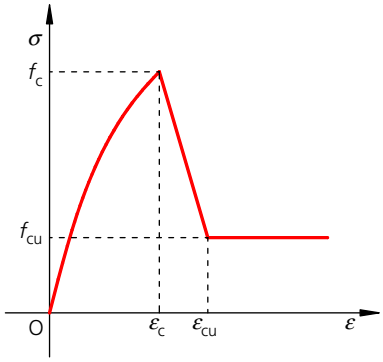

Figure 2. Uniaxial compressive stress–strain curve

in the descending branch of curve, as shown in Figure 2. The expression of the compressive stress–strain curve is

$$2.\quad \sigma_{com} = \begin{cases} f_c\left[k\left(\dfrac{\varepsilon}{\varepsilon_c}\right) + (1-k)\left(\dfrac{\varepsilon}{\varepsilon_c}\right)^2\right] & (\varepsilon \le \varepsilon_c) \\ f_c + (f_{cu} - f_c)\left(\dfrac{\varepsilon - \varepsilon_c}{\varepsilon_{cu} - \varepsilon_c}\right) & (\varepsilon_c < \varepsilon \le \varepsilon_{cu}) \\ f_{cu} & (\varepsilon > \varepsilon_{cu}) \end{cases}$$

where ε_c is the compressive strain at peak stress f_c, which is usually fixed at 0·002 for normal concrete, f_{cu} is the residual stress, ε_{cu} is the strain corresponding to f_{cu} and k is the shape factor of the ascending branch.

Unloading mechanism

Yassin (1994) proposed a cyclic unloading and reloading model for concrete, which is represented by a set of straight lines. On the compressive side of the model, as shown in Figure 3, the degradation of stiffness is such that the reverse extension lines of all reloading lines intersect at a common point (called the reference point R). The reloading line is determined by the connecting line of the historic maximum strain of the monotonic envelope curve and the reference point R, and the slope of the reloading line is recorded as E_r. The

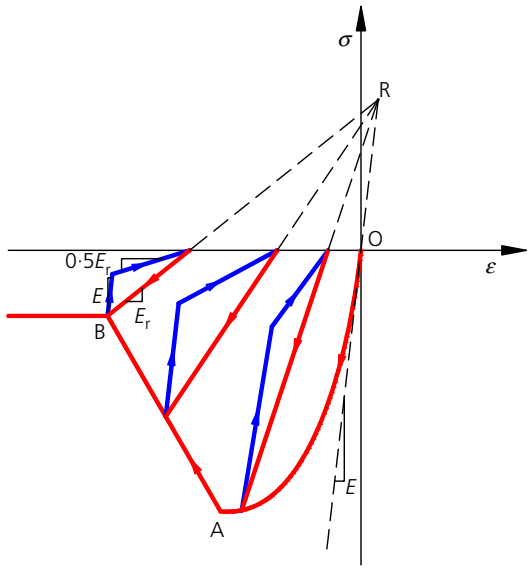

Figure 3. Uniaxial cyclic constitutive model for concrete proposed by Yassin (1994)

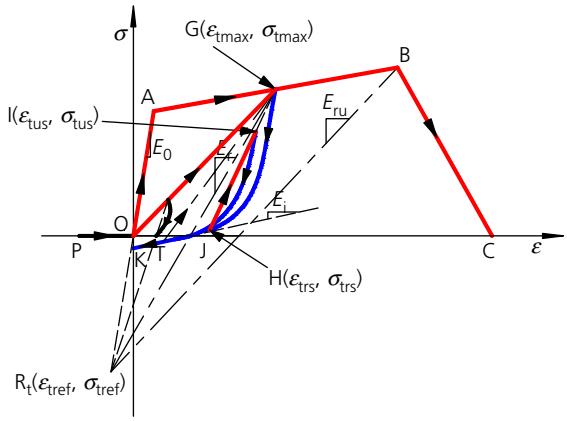

Figure 4. Stress–strain curve of SHCC under cyclic loading in tension

unloading rule follows two straight lines with modulus E and $0{\cdot}5E_r$ respectively. This method of presetting a reference point provides a solution of stiffness degradation of concrete at unloading under different loading histories.

Based on the unique characteristics of SHCCs, the bilinear form of the descending branch in the model proposed by Yassin (1994) was changed into the curved form. In seismic non-linear analysis, partial unloading and reloading often occurs. In the proposed constitutive model, partial unloading and reloading are also considered to accurately model the SHCC material, which means unloading is allowed to start from reloading by partial unloading or from the envelope curves. The detailed unloading and reloading curves in tension and compression are schematically shown in Figures 4 and 5,

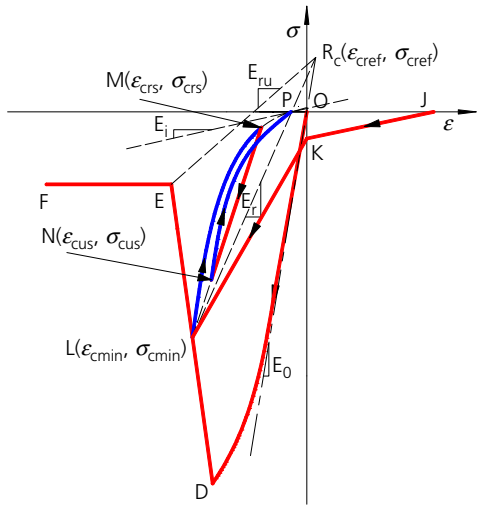

Figure 5. Stress–strain curve of SHCC under cyclic loading in compression

respectively. $R_t(\varepsilon_{tref}, \sigma_{tref})$ and $R_c(\varepsilon_{cref}, \sigma_{cref})$ represent the reference points of unloading and reloading curves in tension and compression, respectively.

To facilitate the use of computer-aided calculations, the unloading curve before reaching the zero-stress axis in tension (lines GH and IJ in Figure 4) and in compression (lines LM and NP in Figure 5) are unified as follows

3. $$\sigma^* = \alpha\varepsilon^* + (1-\alpha)(\varepsilon^*)^p$$

in which

$$\varepsilon^* = \frac{\varepsilon - \varepsilon_0}{\varepsilon_{us} - \varepsilon_0}$$

$$\sigma^* = \frac{\sigma}{\sigma_{us}}$$

$$\alpha = \frac{E_i}{E_r}$$

and p is the power law of ε^*. α and p are introduced to control the shape of the curve, and the values of α and p can be determined through experiment. ε_0 is the residual strain at the point where the stress is reduced to zero and is given by

4. $$\varepsilon_0 = \varepsilon_{us} - \frac{\sigma_{us}}{E_r}$$

	Full reloading	Partial reloading
Tension	$\varepsilon_{us} = \varepsilon_{tmax}$	$\varepsilon_{us} = \varepsilon_{tus}$
	$\sigma_{us} = \sigma_{tmax}$	$\sigma_{us} = \sigma_{tus}$
Compression	$\varepsilon_{us} = \varepsilon_{cmin}$	$\varepsilon_{us} = \varepsilon_{cus}$
	$\sigma_{us} = \sigma_{cmin}$	$\sigma_{us} = \sigma_{cus}$

Table 1. Determination of ε_{us} and σ_{us}

The value of E_r can be determined by the location of the reference points ($R_t(\varepsilon_{tref}, \sigma_{tref})$ in Figure 4 and $R_c(\varepsilon_{cref}, \sigma_{cref})$ in Figure 5). E_r can be calculated from

5. $$E_r = \frac{\sigma_{us} - \sigma_{ref}}{\varepsilon_{us} - \varepsilon_{ref}}$$

in which

$$\sigma_{ref} = \begin{cases} \sigma_{tref} & \text{in tension} \\ \sigma_{cref} & \text{in compression} \end{cases}$$

$$\varepsilon_{ref} = \begin{cases} \varepsilon_{tref} & \text{in tension} \\ \varepsilon_{cref} & \text{in compression} \end{cases}$$

and ε_{us} and σ_{us} are the strain and stress at the unloading point; their values are listed in Table 1.

It is important to note that the strain is regarded as positive in tension and negative in compression for the derivations presented in this study. In Table 1, ε_{tmax} and ε_{cmin} are the maximum experienced tensile strain and the minimum experienced compressive strain as shown in Figures 4 and 5, respectively. σ_{tmax} and σ_{cmin} are the stresses corresponding to ε_{tmax} and ε_{cmin}, respectively. Full reloading means that reloading starts from complete unloading in tension or in compression, such as points $G(\varepsilon_{tmax}, \sigma_{tmax})$ in Figure 4 and $L(\varepsilon_{cmin}, \sigma_{cmin})$ in Figure 5, while partial reloading means that reloading starts from a partial unloading originating in tension or in compression, such as $I(\varepsilon_{tus}, \sigma_{tus})$ in Figure 4 and $N(\varepsilon_{cus}, \sigma_{cus})$ in Figure 5.

The coordinate values of reference points $R_t(\varepsilon_{tref}, \sigma_{tref})$ and $R_c(\varepsilon_{cref}, \sigma_{cref})$ can be determined according to the experimental results. The determination procedure is as follows. The unloading curve at the peak point in tension or in compression is taken, and a secant is drawn to intersect the peak point and the point where the stress is reduced to zero; the slope of this line is E_{ru}. This line is then extended to the intersection with the tangent line at the original point whose slope is E_0, and the intersection is defined as $R_t(\varepsilon_{tref}, \sigma_{tref})$ (or $R_c(\varepsilon_{cref}, \sigma_{cref})$).

Assuming $\gamma = E_{ru}/E_0$, the calculation formula of coordinate values of $R_t(\varepsilon_{tref}, \sigma_{tref})$ (or $R_c(\varepsilon_{cref}, \sigma_{cref})$) is as follows

$$6. \quad \begin{cases} \varepsilon_{ref} = \dfrac{(\sigma_u/E_0) - \gamma\varepsilon_u}{1-\gamma} \\ \sigma_{ref} = E_0\varepsilon_{ref} \end{cases}$$

where

$$\sigma_u = \begin{cases} f_{tl} & \text{in tension} \\ f_{cu} & \text{in compression} \end{cases}$$

and ε_u is the strain corresponding to σ_u.

Reloading mechanism

The reloading curve is simplified to the straight line between the loading point (point H in Figure 4 or point M in Figure 5) to the stress point (point G in Figure 4) corresponding to the maximum strain in the previous load history in tension and the stress point (point L in Figure 5) corresponding to the minimum strain in the previous load history in compression, that is line HI in Figure 4 and line MN in Figure 5. Their expressions are as follows

$$7. \quad \sigma = \sigma_{rs} + (\sigma_m - \sigma_{rs})\frac{\varepsilon - \varepsilon_{rs}}{\varepsilon_m - \varepsilon_{rs}}$$

in which

$$\varepsilon_m = \begin{cases} \varepsilon_{t\,max} & \text{in tension} \\ \varepsilon_{c\,min} & \text{in compression} \end{cases}$$

σ_m is the stress corresponding to ε_m

$$\varepsilon_{rs} = \begin{cases} \varepsilon_{trs} & \text{in tension} \\ \varepsilon_{crs} & \text{in compression} \end{cases}$$

and σ_{rs} is the stress corresponding to ε_{rs}.

Transition between tension and compression

Unloading from a point in the non-linear phase and at the moment of reaching the zero-stress axis, the stress usually does not stay at zero but continues to reduce, which means that the stress state is changed from tension/compression into compression/tension. Kesner *et al.* (2003) gave a typical complete stress–strain hysteresis loop of SHCC from a Y–R loading mode (Yankelevsky and Reinhardt, 1989). They concluded that there were three distinct phases in both the unloading and reloading portions of the complete hoop: the unloading phase comprised initial elastic unloading, cracks closing with low compressive stiffness and cracks closing with increasing compressive stiffness in which the material could again sustain the compression; the reloading phase was composed of initial elastic unloading, crack opening with low stiffness and increasing tensile stiffness with increasing crack opening due to the fibre-bridging effect. In the model of Han *et al.* (2003), the transition effect from tension to compression or from compression to tension was ignored, and they assumed that the behaviour of further unloading started from the initial elastic unloading to the original point.

If SHCC material is loaded from tension to compression, the stress–strain relation is simplified to be bilinear, as shown by lines JK and KL in Figure 5. Point K lies in the axis of stress, which means that the strain at point K is zero and the slope of line JK is E_i. Line KL is the connecting line between point K and point L. If the material is loaded from compression to tension, the stress remains zero while the strain goes back to the original point first. Then, a secant is drawn to intersect the original point and the maximum strain point in the previous load history, as shown by lines PO and OG in Figure 4. The detailed expressions are as follows.

From tension to compression

$$8. \quad \sigma = \begin{cases} E_i(\varepsilon - \varepsilon_0) & (\varepsilon_0 \geq \varepsilon > 0) \\ \dfrac{\varepsilon}{\varepsilon_{c\,min}}(\sigma_{c\,min} + E_i\varepsilon_0) - E_i\varepsilon_0 & (\varepsilon \leq 0) \end{cases}$$

From compression to tension

$$9. \quad \sigma = \begin{cases} 0 & (\varepsilon < 0) \\ \sigma_{t\,max}/\varepsilon_{t\,max} & (\varepsilon \geq 0) \end{cases}$$

During the transition between tension and compression, if unloading or reloading occurs, the stress–strain relation is consistent with the aforementioned models in the Sections 'Unloading mechanism' and 'Reloading mechanism', such as T → G in Figure 4.

SHCC model implementation and validation

SHCC model implementation and coding in OpenSees

OpenSees (2014), a well-recognised open-source platform developed at UC Berkeley and supported by the Pacific Earthquake Engineering Research Center (PEER) and the Network for Earthquake Engineering Simulation (NEES), has been utilised based on object-oriented C++ language source code since the end of the last century. Given that OpenSees is open source with a well-developed fibre element method to perform non-linear structural analysis, the proposed SHCC model was implemented into OpenSees to enable structural simulations. The proposed cyclic model was embedded as new user-defined material in the OpenSees platform, and called SHCC01 based on the C++ language.

			SHCC	
	Concrete	FRC	Common HPFRC	ECC
Fibre	No fibre	Any type; $V_f \leq 2\%$, $d_f \approx 500$ μm (steel)	Mostly steel; usually $V_f > 5\%$, $d_f \approx 150$ μm	Tailored, polymer fibres most suitable; usually $V_f < 2\%$, $d_f < 50$ μm
Matrix	Coarse aggregates used	Coarse aggregates used	Fine aggregates used	Controlled for matrix toughness and initial flaw size; fine sand used
Tensile behaviour	Strain-softening	Strain-softening	Strain-hardening	Strain-hardening
Tensile strain capacity	≈0·01%	≈0·10%	<1·5%	>3%
Applicability of proposed model	No	No	Yes	Yes

Table 2. Applicability of proposed model to cement-based materials

Determination of model parameters

The proposed constitutive model is suitable for cement-based materials with tensile strain-hardening behaviour, including high-performance fibre reinforced concrete (HPFRC) and ECCs (Li, 2002). Normal concrete and fibre reinforced concrete (FRC) with tensile strain-softening behaviour are not suitable for the model. The applicability of the proposed model to several types of cement-based materials is listed in Table 2.

The tensile failure envelope of SHCCs can be determined based on experimental observations. The first cracking stress (f_{t0}) approximately varies from 2·0 MPa to 5·0 MPa and the tensile strength (f_{t1}) ranges from $1{\cdot}2f_{t0}$ to $1{\cdot}5f_{t0}$. However, the relationship between tensile strength (f_{t1}) and compressive strength (f_c) needs to be discussed further.

For the compressive failure envelope of SHCCs, Han *et al.* (2003) assumed that the envelope was linear up to a peak compressive stress, meaning k in Equation 2 equals 1·0, and the softened branch was also linear until the strain reached the ultimate compressive strain. Through a series of compressive tests on SHCC material, f_{cu} in Equation 2 is proposed to vary from $0{\cdot}2f_c$ to $0{\cdot}3f_c$, ε_{cu} is taken as $1{\cdot}2\varepsilon_c$ to $1{\cdot}5\varepsilon_c$, and k varies from 1·0 to 2·0.

Based on test results reported by Kesner *et al.* (2003), the suggested model parameters in the aforementioned unloading mechanism are listed in Table 3.

	α	p	γ
Tension	0·2	5	0·2
Compression	0·2	3	0·35

Table 3. Model parameters

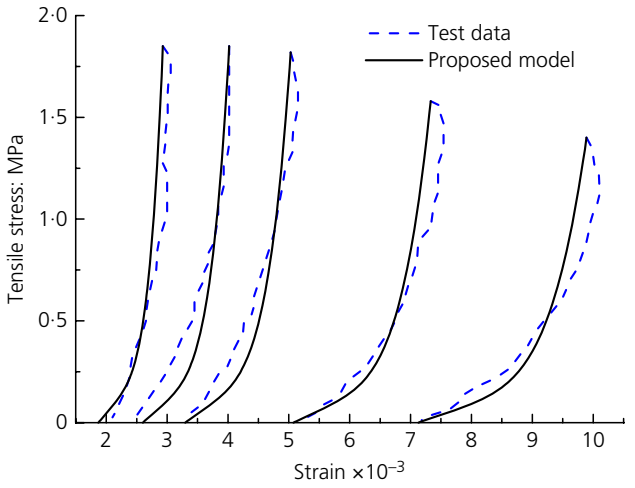

Figure 6. Comparison of tested and simulated unloading curves in tension

Experimental verification at material level

To evaluate the validity of the proposed cyclic constitutive model of SHCC, experimental observations at the material level (Kesner *et al.*, 2003) were selected for comparison with the results simulated by the model SHCC01 in OpenSees. The loading and unloading curves are plotted for tension and compression in Figures 6 and 7 for a better comparison of the material tests and the proposed model. The simulation results of the proposed model show very good correspondence with the test data.

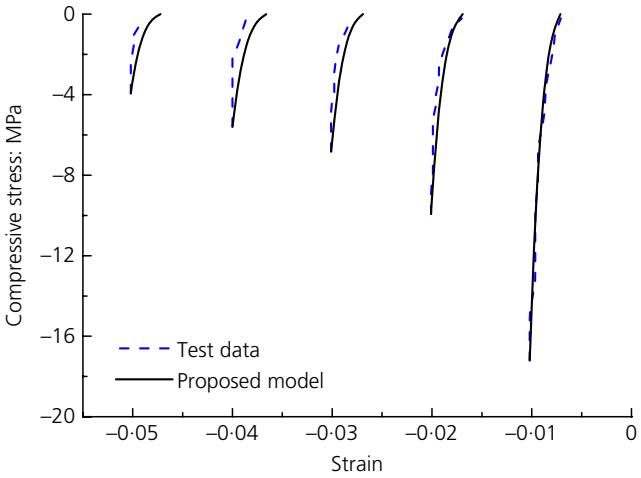

Figure 7. Comparison of tested and simulated unloading curves in compression

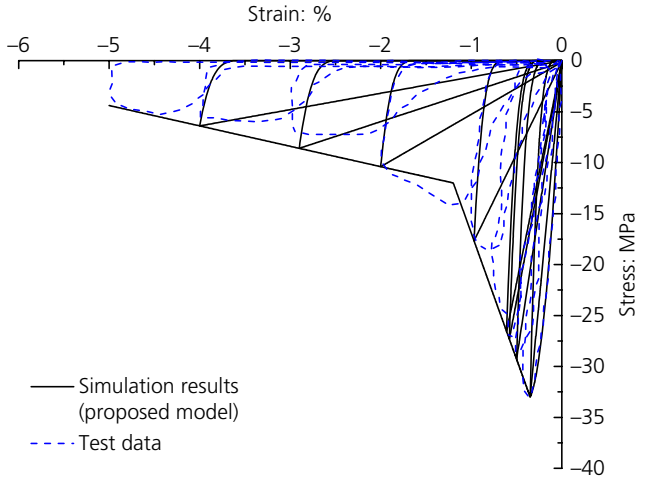

Figure 9. Comparison of simulation results of proposed model with test data in compression region

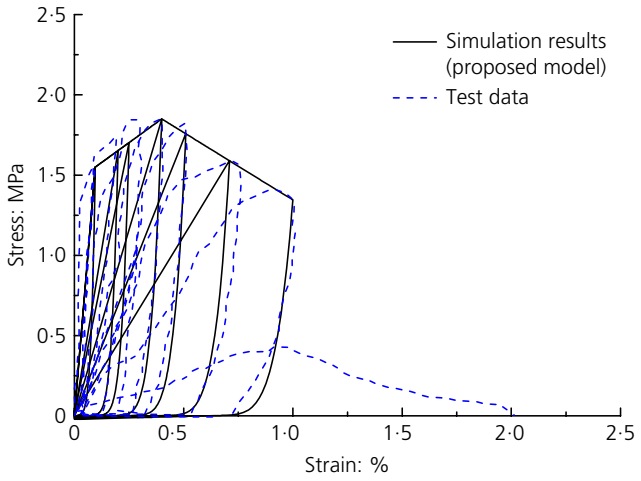

Figure 8. Comparison of simulation results of proposed model with test data in tension region

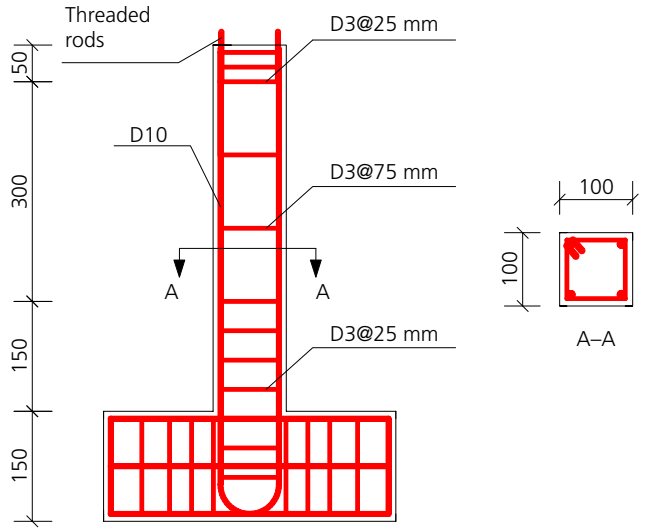

Figure 10. Geometry and reinforcement details (dimensions in mm)

Comparison of the results under cyclic loading and unloading in tension and compression regions are shown in Figures 8 and 9, respectively. Figures 8 and 9 indicate that the proposed SHCC constitutive model can simulate the experimental behaviour of SHCC under cyclic tensile or compressive loading (e.g. strain-hardening, pinching effect, unloading and reloading response, strength and stiffness degradation) with reasonable accuracy, which means that the unloading and reloading mechanisms presented in this study reflect the actual behaviour of SHCC material well.

Experimental verification at member level

To assess the validity of the proposed cyclic constitutive model of SHCC at the member level, the cyclic response of a reinforced ECC (R/ECC) cantilever beam experiment reported by Fischer and Li (2003) was simulated using SHCC01 in OpenSees. The geometry and reinforcement details of the cantilever beam specimen are shown in Figure 10. The cantilever beam was tested under cyclic horizontal forces.

The R/ECC cantilever beam was simulated using a fibre-based non-linear beam–column finite element with two-dimensional sections in OpenSees. The cross-section of the beam was divided into fibres, which forms the basis of distributed inelasticity models. Each fibre can then be assigned a different material model. The proposed SHCC01 material model was used for the SHCC in the beam and the Steel02 material

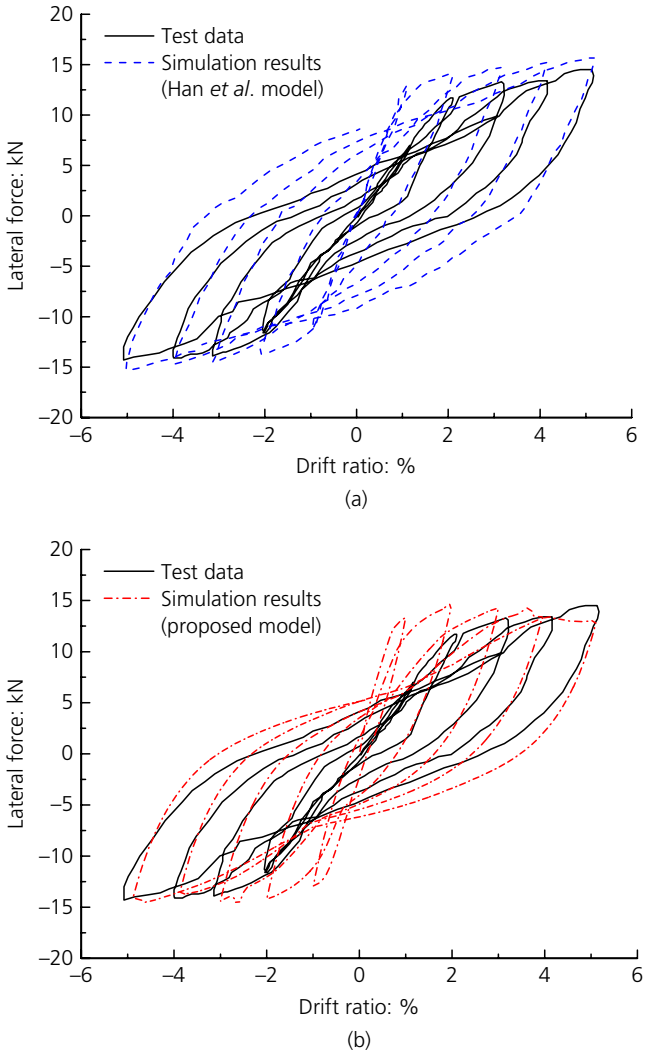

Figure 11. Comparison of test hysteresis loops with (a) model of Han *et al.* (2003) and (b) proposed model

model was used for the reinforcement. It should be noted that the effect of confinement of transverse reinforcement on the hysteretic behaviour of specimens was insignificant in the experimental observations of Fischer and Li (2002, 2003). This is because the PVA fibres serve as the self-confinement in SHCC, and the influence of lateral compression on the uniaxial compression behaviour is not obvious. An assumption in this study was thus to ignore the effect of confinement from the transverse reinforcement.

For the sake of comparison with the model of Han *et al.* (2003), the model parameters in this study were kept identical to those presented by Han *et al.* and the loading schemes were also the same. Figure 11 shows a comparison of the reversed cyclic test results with simulations from the proposed model and the model of Han *et al.* (2003).

The comparisons in Figures 11(a) and 11(b) indicate that the initial stiffness of the calculation curve by the proposed model is greater than the test results, and slightly greater than the results of the model of Han *et al.* After the cantilever beam enters the plastic state, compared with the simulation results from Han *et al.*'s model, the proposed model shows more consistency with the test data. Furthermore, the proposed model displays more distinct pinching, more closely matching the experimental results, as a result of accounting for the transition from tension to compression or from compression to tension as described earlier in the paper.

Conclusions

A cyclic constitutive model for strain-hardening cementitious composite (SHCC) material was proposed. Based on a comparison of numerical and experimental studies, the following conclusions can be drawn.

(*a*) In the proposed cyclic constitutive model for SHCCs, the ascending branch of the compressive envelope curve was developed using the form of a parabolic curve, while the descending branch adopted the bilinear form. A trilinear form was used to simulate the ascending, strain-hardening and descending branches of the tensile stress–strain curve. Using the method of setting a reference point, the characteristics of the unloading and reloading process were determined, with consideration of the partial unloading–reloading scheme. The transition between tension and compression was also considered in the cyclic model development.

(*b*) The proposed cyclic constitutive model was implemented into the OpenSees platform for structural simulations. The accuracy of the proposed model was verified through unloading and reloading experiments of SHCC at the material level. The results of the comparative analysis indicate that the proposed model captures the most distinct mechanical characteristics of SHCC material, such as strain-hardening, the pinching effect, unloading and reloading response and strength and stiffness degradation with reasonable accuracy.

(*c*) Further calibration of the proposed model was carried out through a comparison with a cantilever beam test. The simulation results demonstrate that a fibre-based non-linear beam–column model embedded with the proposed model can characterise the hysteretic behaviour with reasonable accuracy. Compared to the model of Han *et al.* (2003), the proposed model can capture the pinching effect, which is more similar to the behaviour of SHCC members entering the plastic state.

(*d*) The proposed model can be applied to a fibre-based non-linear beam–column element for simulating the behaviour of flexural members and the global response of complete structural systems constructed with SHCC materials. The fibre-based finite-element method can also

be applied to pushover analysis and dynamic time history analysis, and consequently to assess the seismic performance of SHCC structures.

Acknowledgement

The authors acknowledge funding support from the National Natural Science Foundation of China (grant 51208093), the Doctoral Program of the Ministry of Education, China (grant 20120092120021), the State Key Laboratory of High Performance Civil Engineering Materials (2012CEN006) and the Priority Academic Program Development of Jiangsu Higher Education Institutions. The authors also thank Professor Jianzhong Liu and Mr Gong Cui of the Jiangsu Research Institute of Building Science Co., Ltd, China, for their advice.

REFERENCES

Bahn BY and Hsu CTT (1998) Stress–strain behavior of concrete under cyclic loading. *ACI Materials Journal* **95(2)**: 178–193.

Elnashai AS, Papanikolaou VK and Lee D (2010) *Zeus NL – A System for Inelastic Analysis of Structures. User's Manual*. Mid-America Earthquake (MAE) Center, Department of Civil and Environmental Engineering, University of Illinois at Urbana-Champaign, Urbana, IL, USA.

Fischer G and Li VC (2002) Effect of matrix ductility on deformation behavior of steel-reinforced ECC flexural members under reversed cyclic loading conditions. *ACI Structural Journal* **99(6)**: 781–790.

Fischer G and Li VC (2003) Deformation behavior of FRP reinforced ECC flexural members under reversed cyclic loading conditioned. *ACI Structural Journal* **100(1)**: 25–35.

Fukuyama H, Matsuzaki Y, Nakano K and Sato Y (1999) Structural performance of beam elements with PVA-ECC. In *Proceedings of the 3rd International Rilem Workshop on High Performance Fiber Reinforced Cement Composites* (Reinhardt HW and Naaman AE (eds)). RILEM publications SARL, Mainz, Germany, pp. 531–541.

Gencturk B and Elnashai AS (2013) Numerical modeling and analysis of ECC structures. *Materials and Structures* **46(4)**: 663–682.

Han TS, Feenstra PH and Billington SL (2003) Simulation of highly ductile fiber-reinforced cement-based composite components under cyclic loading. *ACI Structural Journal* **100(6)**: 749–757.

Hognestad E, McHenry D and Hanson NW (1955) Concrete stress distribution in ultimate strength design. *Journal of the American Concrete Institute* **27(4)**: 455–479.

Hou LJ, Xu SL and Zhang XF (2012) Toughness evaluation of ultra-high toughness cementitious composite specimens with different depths. *Magazine of Concrete Research* **64(12)**: 1079–1088, http://dx.doi.org/10.1680/macr.11.00186.

Keoleian GA, Kendall A, Dettling JE *et al.* (2005) Life cycle modeling of concrete bridge design: comparison of engineered cementitious composite link slabs and conventional steel expansion joints. *Journal of Infrastructure Systems* **11(1)**: 51–60.

Kesner KE and Billington SL (2001) Investigation of ductile cement based composites for seismic strengthening and retrofit, fracture mechanics of concrete structures. In *Proceedings of the 4th International Conference on Fracture Mechanics of Concrete and Concrete Structures* (Borst RD, Mazars J, Pijaudier-Cabot G and Van Mier J (eds)). Balkema, Cachan, France, pp. 65–72.

Kesner K and Billington SL (2005) Investigation of infill panels made from engineered cementitious composites for seismic strengthening and retrofit. *Journal of Structural Engineering* **131(11)**: 1712–1720.

Kesner KE, Billington SL and Douglas KS (2003) Cyclic response of highly ductile fiber-reinforced cement-based composites. *ACI Materials Journal* **100(5)**: 381–390.

Kojima S, Sakata N, Kanda T and Hiraishi T (2004) Application of direct sprayed ECC for retrofitting dam structure surface – application for Mitaka-Dam. *Concrete Journal of the Japan Concrete Institute* **42(5)**: 135–139.

Lee BY, Lee Y, Kim JK and Kim YY (2010) Micromechanics-based fiber-bridging analysis of strain-hardening cementitious composite accounting for fiber distribution. *Computer Modeling in Engineering & Sciences* **61(2)**: 111–132.

Li VC (2002) Advances in ECC research. In *Concrete: Material Science to Applications*. ACI, Farmington Hills, MI, USA, SP 206-23, pp. 373–400.

Li VC and Leung CKY (1992) Steady state and multiple cracking of short random fiber composites. *Journal of Engineering Mechanics ASCE* **188(11)**: 2246–2264.

Li VC, Stang H and Krenchel H (1993) Micromechanics of crack bridging in fiber reinforced concrete. *Materials and Structures* **26(162)**: 486–494.

Li VC, Wu C, Wang SX, Ogawa A and Saito T (2002) Interface tailoring for strain-hardening polyvinyl alcohol-engineered cementitious composite (PVA-ECC). *ACI Materials Journal* **99(9)**: 463–452.

Maruta M, Kanda T, Nagai S and Yamanoto Y (2005) New high-rise RC structure using precast ECC coupling beam. *Concrete Journal of the Japan Concrete Institute* **43(11)**: 18–26.

OpenSees (2014) *Open System for Earthquake Engineering Simulation*. See http://opensees.berkeley.edu/ (accessed 02/03/2016).

Parra-Montesinos G and Wight JK (2000) Seismic response of exterior RC column-to-steel beam connections. *Journal of Structural Engineering ASCE* **126(10)**: 1113–1121.

Yankelevsky DZ and Reinhardt HW (1989) Uniaxial behavior of concrete in cyclic tension. *Journal of Structural Engineering ASCE* **115(1)**: 166–182.

Yassin M (1994) *Nonlinear Analysis of Prestressed Concrete Structures under Monotonic and Cyclic Loading*. PhD thesis, University of California, Berkeley, CA, USA.

Yun HD, Yang IS, Kim SW *et al.* (2007) Mechanical properties of high-performance hybrid-fibre-reinforced cementitious composites (HPHFRCCs). *Magazine of Concrete Research* **59(4)**: 257–271, http://dx.doi.org/10.1680/macr.2007.59.4.257.

Yun HD, Kim SW, Lee YO and Rokugo K (2011) Tensile behavior of synthetic fiber-reinforced strain-hardening cement-based composite (SHCC) after freezing and thawing exposure. *Cold Regions Science and Technology* **67(1–2)**: 49–57.